Ab Initio Molecular Orbital Study of the Insertion of H_2 into POSS Compounds 2: The Substituent Effect and Larger Cages

Takako Kudo*

Department of Chemistry and Chemical Biology, Graduate School of Engineering, Gunma University, Kiryu 376-8515, Japan

Received: May 14, 2009; Revised Manuscript Received: August 14, 2009

The insertion of H_2 molecules into the substituted cubic oligomeric silsesquioxanes (POSS), R_8T_8, $[RSiO_{1.5}]_8$; R = F, Li, CH_3, and SiH_3, was investigated in comparison with the parent H compound, $[HSiO_{1.5}]_8$, at the HF and second order perturbation theory (MP2) methods. Also investigated were the stabilities of isomers of larger size of POSS, T_{14} ($[HSiO_{1.5}]_{14}$), and T_{16} ($[HSiO_{1.5}]_{16}$), and the same reaction for them. Furthermore, the possibility of the encapsulation of multiple H_2 molecules is discussed for T_{14} and T_{16}.

Introduction

For many years, polyhedral oligomeric silsesquioxanes (POSS) with cage structures have been the focus of considerable experimental and theoretical interest because of their wide variety of practical uses.[1] As seen from the molecular formula, T_n, $[RSiO_{1.5}]_n$; n = 4,6,8,10,12 ..., they have the potential to be inorganic/organic nanocomposites by introducing various kinds of substituents (R) on the silicon atoms of the frameworks, suggesting the possibility of rather easily developing newer functionalities of these compounds by the substituent effect.[2]

On the other hand, one recent exciting topic is the encapsulation of some atoms and ions including transition metals and small molecules in the cavity of these compounds.[3] Especially for F^- ions, both experimental and theoretical chemists have demonstrated a high level of interest by devoting studies to the structure, stability of the isomers, ion mobility, and mass or NMR spectroscopy and so on. Among them, Anderson et al.[3j] suggested, in their study on the structure and ion mobility of various kinds of F^- encapsulated POSS, that the R groups on the silicon atoms play important role for the properties of the F^- encapsulated R_8T_8. Incidentally, we also have been recently working on the incorporation of F^- into the titanium analogs of POSS, $[HTiO_{1.5}]_n$, but they will be presented in another work.[4]

In the past several years, the authors have studied many aspects of POSS and related compounds.[5] From a couple of years ago, we have started the analysis of the mechanism of H_2 insertion into POSS and metal analogs with regard to the future development of molecular sieves and H_2 storage.[3i] In continuing our investigations, we are presenting here the substituent (R) effect on the H_2 encapsulation in the most common POSS, T_8 ($[HSiO_{1.5}]_8$). Furthermore, for the H_2 storage, the larger POSS, such as T_{14} ($[HSiO_{1.5}]_{14}$) and T_{16} ($[HSiO_{1.5}]_{16}$), seem to be interesting targets for examination. Therefore, the H_2 encapsulating reaction for them are also discussed.

Computational Methods

The geometries of the substituted T_8, (R_8T_8), $[RSiO_{1.5}]_8$; R = H, F, Li, CH_3, and SiH_3, and the related molecules of interest have been fully optimized at the Hartree−Fock and second order perturbation (MP2)[6] levels of theory, using the SBKJC effective core potential[7] and the TZV(d,p)[8] basis set. After that, in order to get more reliable energetics, the single point energy calculations at the MP2 level of theory on the HF/TZV(d,p) optimized geometries were performed, except for larger T_{14} and T_{16} systems. For these, even the MP2 single point calculations with the TZV(d,p) basis set are too big to treat here, so the MP2/SBK are the highest levels of calculation in the present study.

All optimized structures were characterized as minima or transition states by calculating and diagonalizing the corresponding Hessian matrix of energy second derivatives.

All calculations were performed with the GAMESS electronic structure code.[9]

TABLE 1: Geometries (Å and degrees) of $[RSiO_{1.5}]_8$ (R = H, CH_3, SiH_3, F, and Li) at the HF/TZV(d,p) and MP2/SBK[a] Levels of Theory

R	*r*(Si−O)	*r*(Si−R)	<Si−O−Si	<O−Si−O
H	1.624(1.700)	1.455(1.483)	150.5(152.4)	108.4(107.4)
CH_3	1.628(1.704)	1.852(1.886)	150.9(152.4)	108.2(107.4)
SiH_3	1.631(1.711)	2.349(2.376)	151.5(152.4)	107.9(107.4)
F	1.611(1.678)	1.559(1.672)	149.5(153.4)	108.9(106.9)
Li	1.650(1.746)	2.518(2.514)	153.5(153.0)	106.9(107.0)

[a] The values are in parentheses.

Results and Discussion

1. Substituent Effect on H_2 Insertion into T_8. First, we summarize some geometrical parameters of the optimized structures of substituted T_8, (R_8T_8), $[RSiO_{1.5}]_8$; R = H, F, Li, CH_3, and SiH_3 (see Table 1). In all cases, the MP2/SBK level predicts SiO bond length longer than that at the HF/TZV(d,p) level as seen in our previous results.[3i] Furthermore, the framework of the cage shrinks in the fluorine substituted T_8 because of the shorter SiO bond length compared with those in others while the bond lengthens in $(SiH_3)_8T_8$ and Li_8T_8, especially in the latter. However, the CH_3 group does not have a serious effect on the size of the cage. The effect of fluorine may be explained from the fact that the large negative charges on the fluorine atoms enhance the charge polarization on the siloxane bonds and strengthen the bonds by electrostatic interaction. Contrary to the Si−O distance, the Si−O−Si and O−Si−O bond angles are not seriously affected by the substituents.

* To whom correspondence should be addressed. E-mail: tkudo@sci.gunma-u.ac.jp.

10.1021/jp904488s CCC: $40.75
Published on Web 10/12/2009

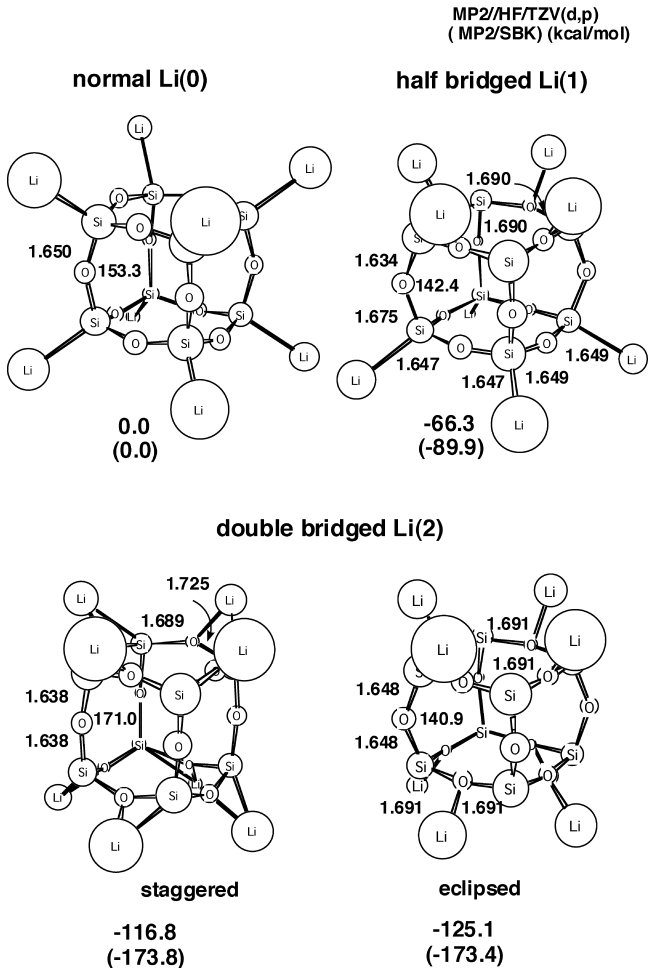

Figure 1. HF/TZV(d,p) optimized geometries (Å and degrees) of the four isomers of Li_8T_8 and the relative energies (kcal/mol) at the MP2/TZV(d,p)//HF/TZV(d,p) and MP2/SBK levels of theory.

On the other hand, the effect of lithium is noteworthy. The structures in Figure 1 are the four isomers of them. The "normal" structure (Li(0)), similar to all other substituted T_8, is least stable, while the structures (Li(1) and Li(2)) where the lithium atoms bridge over the silicon and oxygen atoms are much more stable than Li(0). This behavior of lithium atoms makes the SiO bonds weaker and longer than those in the normal structure. This is not surprising when one considers the large plus charge on lithium.

The "half-bridged" isomer (Li(1)) has one lithium-bridged face, while the "double-bridged" isomer (Li(2)) has such faces at the bottom and top. Furthermore, for the "double bridged" isomer, we have located two conformers, eclipsed and staggered with respect to the top and bottom faces, at all levels of theory employed herein (Scheme 1). For the eclipsed conformation, lithium atoms perfectly moved on the oxygen in both faces with almost D_{4h} symmetry at the HF/TZV(d,p) level. Another difference between the two conformers is the shape of the side (D_4) faces. Compared to the normal D_4 ring, the D_4 in the staggered form is elongated to the vertical direction, whereas in the eclipsed form, it has a flat square structure similar to that of the "half-bridged" isomer because of the changes of the Si—O—Si bond angles in the vertical direction. The staggered conformer of Li(2) is slightly more stable than the eclipsed form at the HF/SBK and MP2/SBK levels, but at the HF/TZV(d,p) level, the stability has turned to be opposite, though both conformations still have the equilibrium structures. Finally, the eclipsed conformer is more stable than another conformer by 8.3 kcal/mol at the MP2/TZV(d,p)//HF/TZV(d,p) level.

These four isomers are found to isomerize each other via the transition states for the 1,2-transfer of lithium atoms, but the "double-bridged" isomers are presumed to be the only possible existing structures from the large stabilization energies relative to other two isomers.

Now, let us move to the discussion on the H_2 insertion into the substituted T_8. The HF/TZV(d,p) optimized structures of the transition states for H_2 insertion and the corresponding inclusion complexes for F_8T_8, $(CH_3)_8T_8$, and $(SiH_3)_8T_8$ are displayed in Figure 2. As clearly shown in Table 2, the geometrical changes on the H_2 insertion in all cases are similar and quite local phenomena. On the face upon which the insertion of the hydrogen molecule takes place in the transition state, the Si—O distance increases, the Si—O—Si bond angle gets narrow and the O—Si—O bond angle is expanded. However, the geometry of the other faces is almost unchanged. After the encapsulation of a hydrogen molecule, however, the changes in the transition state have disappeared but only the side Si—O distance increases because of the impurity, suggesting that the cage size becomes bigger compared to the empty cage. These trends are also seen in the original T_8 and other metal substituted T_8 in our previous work.[3i]

In Figure 3 the HF/TZV(d,p) optimized structures of the transition state and the inclusion complex of the three isomers of Li_8T_8 are displayed. Similar geometric changes as those found in the other substituted T_8 are observed here. For the doubly bridged isomers, we have tried to locate the transition state and the inclusion complex both for the eclipsed and staggered conformers, since both are equilibrium structures and have

SCHEME 1: Conformers of Li(2)

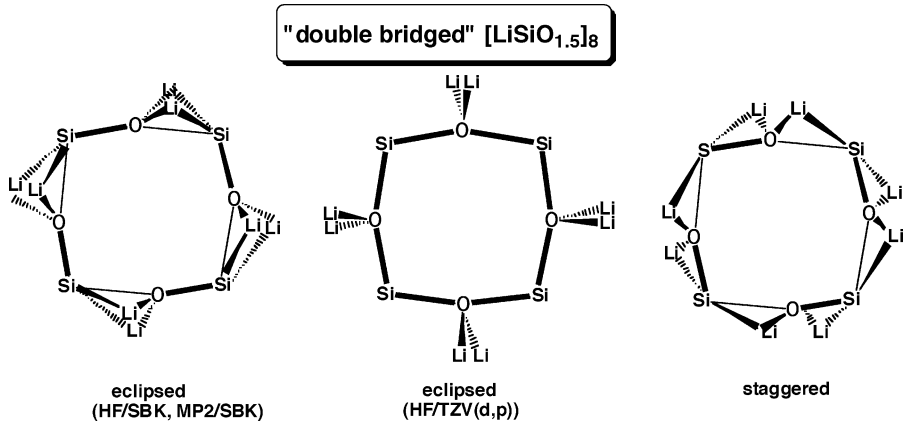

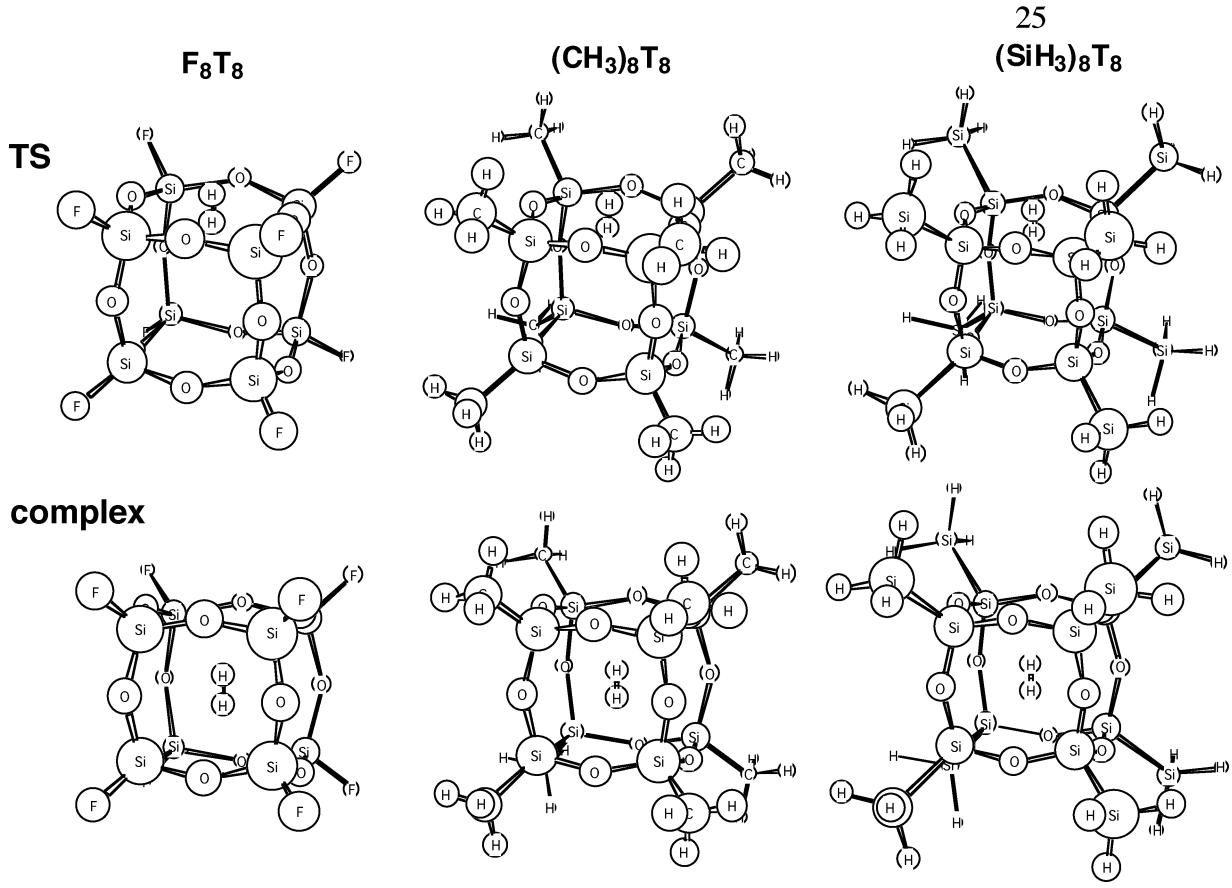

Figure 2. HF/TZV(d,p) optimized structures of the transition states (upper) and the inclusion complexes (lower) for the H_2 insertions into F_8T_8, $(CH_3)_8T_8$, and $(SiH_3)_8T_8$.

TABLE 2: Geometries (Å and degrees) of the Transition Structures for the H_2 Insertion into the $[RSiO_{1.5}]_8$ (R=H, CH_3, SiH_3, F, and Li) and the Inclusion Complexes at the HF/TZV(d,p) Levels of Theory

	R = F		R = CH_3		R = SiH_3	
	TS	complex	TS	complex	TS	complex
top *r*(Si—O)	1.653	1.616	1.672	1.633	1.677	1.637
<Si—O—Si	143.0	150.0	145.0	151.5	145.4	152.0
<O—Si—O	116.7	108.8	115.8	108.0	115.6	107.8
side *r*(Si—O) up	1.609	1.615	1.625	1.632	1.629	1.636
r(Si—O) down	1.610	1.615	1.627	1.632	1.630	1.636
<Si—O—Si	154.2	147.7	154.7	149.2	155.3	149.8
bottom r(Si—O)	1.610	1.616	1.628	1.633	1.631	1.637
<Si—O—Si	147.8	150.0	149.8	151.5	150.4	152.0
<O—Si—O	109.0	108.8	108.2	108.0	107.9	107.8
r(H—H)	0.695	0.705	0.694	0.706	0.694	0.706
	R = Li(0)		R = Li(1)		R = Li(2)	
	TS	complex	TS	complex	TS	complex
top *r*(Si—O)	1.704	1.657	1.726−1.816	1.694−1.722	1.725−1.815	1.694−1.722
<Si—O—Si	145.0	153.7	144.4	156.0	144.8	157.6
<O—Si—O	114.9	106.9	112.7	104.0	113.0	104.2
side *r*(Si—O) up	1.644	1.656	1.625	1.634	1.637	1.646
r(Si—O) down	1.646	1.656	1.657	1.672	1.636	1.646
<Si—O—Si	162.2	151.5	171.7	152.9	176.7	155.5
bottom r(Si—O)	1.652	1.657	1.652	1.655	1.689−1.725	1.694−1.722
<Si—O—Si	149.8	153.7	148.5	156.2	148.6	157.6
<O—Si—O	107.0	106.9	107.2	106.8	104.3	104.2
r(H—H)	0.694	0.707	0.698	0.708	0.698	0.709

similar stability. However, we have obtained only one set of them as shown in the figure. As mentioned before, the eclipsed form has the flat D_4 faces on the side. The structure does not seem to be comfortable for the hydrogen molecule encapsulated in the cage. Therefore, the cage may change to the staggered form during the H_2 insertion process, even if the first conformation of the cage is the eclipsed. That is the reason why we got the unique structure for the transition state and the inclusion complex. We have mentioned that the insertion reaction is quite the local phenomenon in the previous and present studies, but

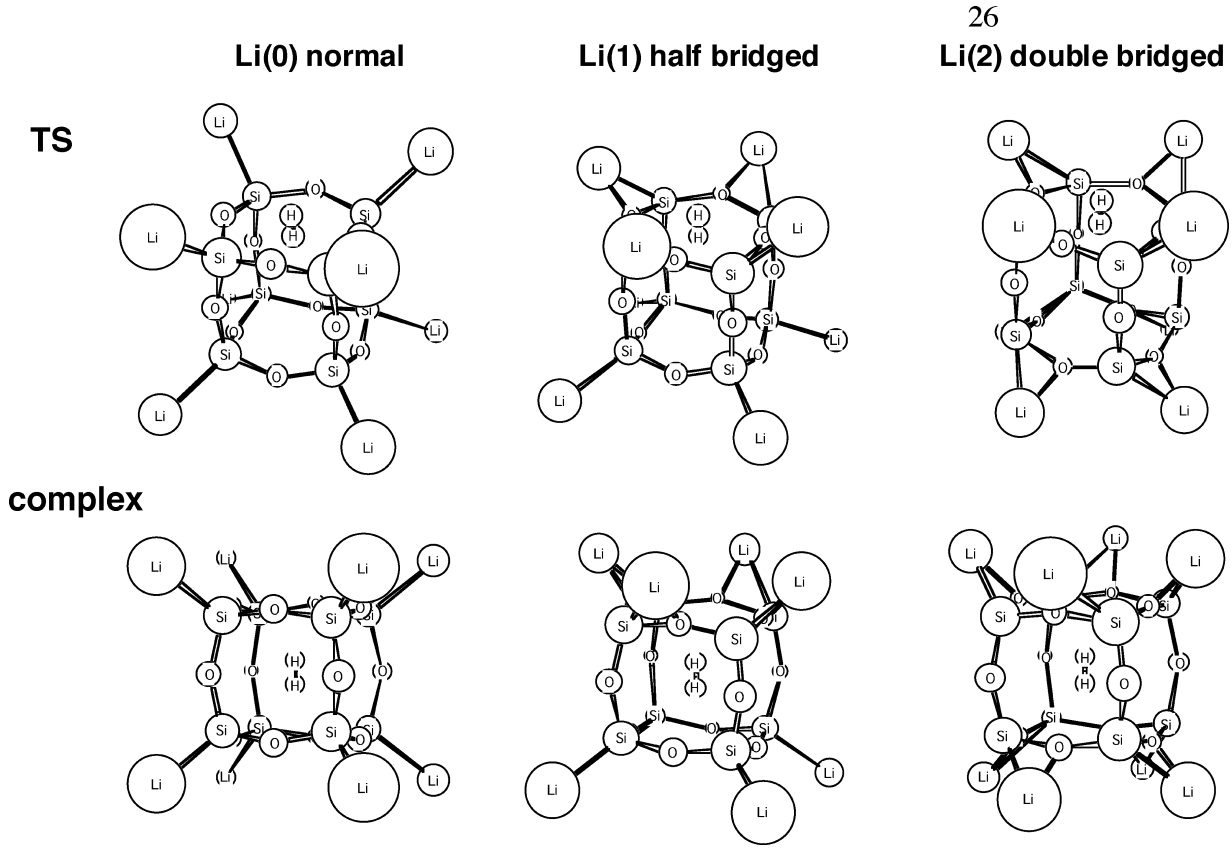

Figure 3. HF/TZV(d,p) optimized structures of the transition states (upper) and the inclusion complexes (lower) for the H_2 insertions into the three isomers of Li_8T_8.

this is an exceptional case where the insertion has affected the whole structure of the cage. This result also suggests that the position of lithium atoms in the "double-bridged" isomers is quite changeable, as expected.

As Table 2 shows, the bond length of the H_2 in the transition state is shorter than that in the complex in all cases. The bond length in the transition state and the complex of the H analog is 0.695 Å and 0.706 Å, respectively, so the substituents examined here at least have little effect on the geometry of the H_2 molecule. Incidentally, the bond distance of a free H_2 molecule was optimized to be 0.734 Å at the HF/TZV(d,p) level, suggesting that the bond tends to shrink on the encapsulation in T_8.

The energy barrier and the stabilization of the inclusion complexes are depicted in Table 3. The energy barrier for the insertion is lower than the H analog in all substituted T_8, with the exception of the fluorine analogue. It is obvious that the size of the face (D_4 ring) has a strong effect on the insertion, as we found in the previous study.[3i] The energy barrier for the lithium compounds are markedly lower than others as expected from the geometries mentioned above. The barrier for the "double-bridged" lithium compound is only 70% of H-T_8 so the insertion is expected to take place very easily compared to the original H analog.

On the other hand, the stabilization energy of the inclusion complex is affected with the size of cage. This is also suggested in our previous study.[3i] The least stable complex is formed with the F_8T_8, while the most stable one is the complex of the "double-bridged" lithium cage and H_2 molecule. The MP2/SBK level of theory has given similar values to those at the MP2/TZV(d,p).

At the end of this section, we will mention the charge transfer between the incorporated H_2 molecule and the substituted T_8.

TABLE 3: Energy Barriers (kcal/mol) for the Insertion of H_2 into $[RSiO_{1.5}]_8$ (R = H, CH_3, SiH_3, F, and Li) and the Energies of the Inclusion Complex (kcal/mol) Relative to the Reactants at the HF/TZV(d,p), MP2/SBK, and MP2/TZV(d,p)//HF/TZV(d,p) Levels of Theory

	energy barrier			stabilization energy of the complex		
R	HF/TZV(d,p)	MP2/SBK	MP2/TZV(d,p)[a]	HF/TZV(d,p)	MP2/SBK	MP2/TZV(d,p)
H	93.8	72.1	74.7	26.7	17.1	15.0
CH_3	93.1	71.1	73.3	26.3	16.1	14.3
SiH_3	92.0	68.5	71.7	25.8	15.0	13.3
F	96.5	77.8	76.8	27.8	18.3	15.4
Li (1)	74.0	45.0	58.7	22.3	10.5	12.2
Li (2)[a]	71.7	44.5	53.6	19.5	10.1	6.0

[a] The empty cage has the staggered conformation.

The Mulliken charge on the H_2 in T_8 is calculated to be −0.2018 at the HF/TZV(d,p) level despite the fact that H_2 is an electrically neutral molecule. This means that the charges on the cage move slightly to the H_2 molecule. The absolute value may be changeable depending on the levels of theory, so we will focus on the relative value. In F_8T_8, H_2 has −0.2256 while it is −0.0964 in the "double-bridged" Li analog, suggesting that by the electron-withdrawing group (F) the H_2 molecule wears more negative charge, while it becomes more electrically positive by the electron-releasing group (Li) compared to the H analog of T_8.

2. H_2 Insertion into T_{14} and T_{16}. Before discussing the H_2 insertion in T_{14} and T_{16}, it may be interesting to know the structure and stability of these compounds. Following the previous studies for larger POSS, T_{14} and T_{16},[10] we have located three isomers for respective POSS, as displayed in Figures 4

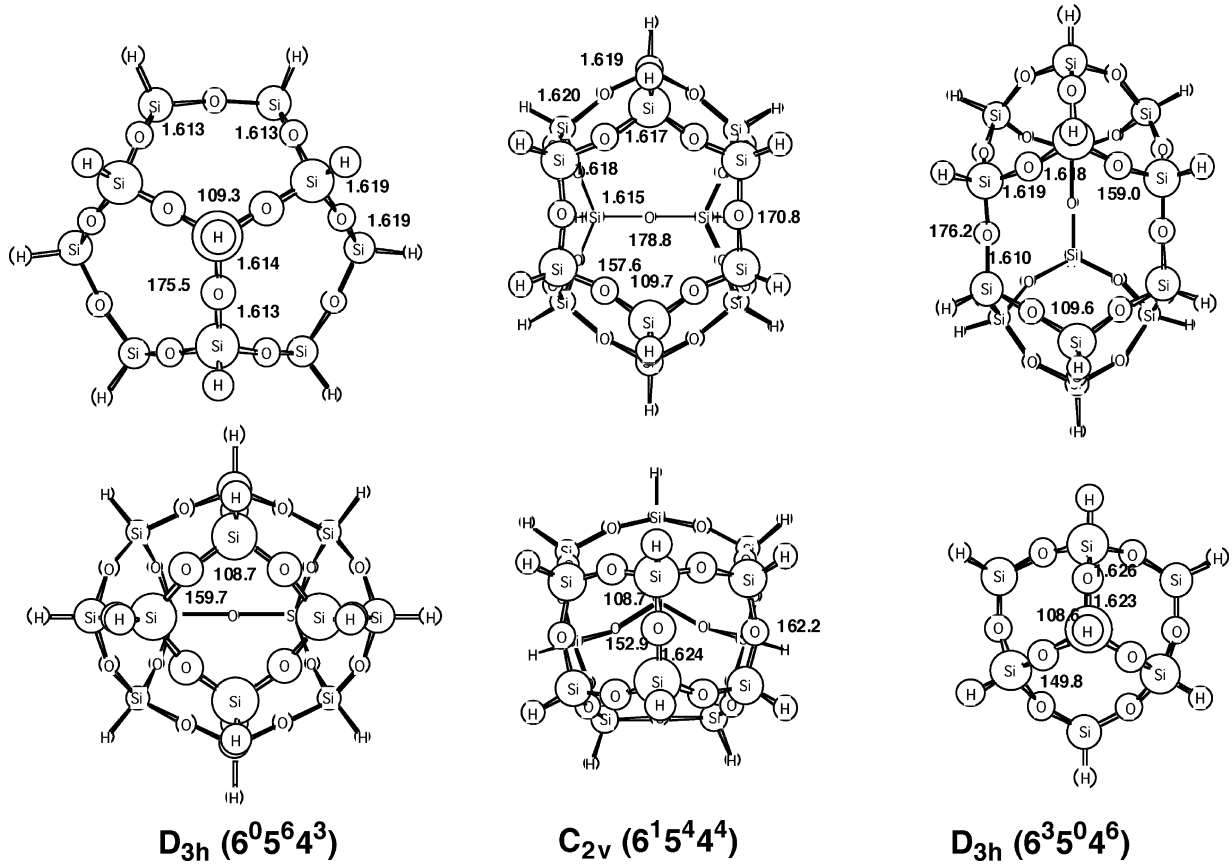

Figure 4. HF/TZV(d,p) optimized geometries (Å and degrees) of the three isomers of T_{14} in two different views.

and 5. The $6^n5^l4^m$ means that the cage structure consists of $n \times 6$ membered ring (12-membered ring if oxygen atoms were included), $l \times 5$ membered ring (10 membered ring), and $m \times 4$ membered rings (8-membered ring). It is obvious from the figures that the ring consisting of the cages becomes large, the Si—O distance decreases, and the Si—O—Si bond angle becomes linear. These trends are similar to those found for the smaller size of POSS,[11] the titanium analog of POSS,[5e] and cyclic siloxane compounds (D_n).[12]

The relative stabilities of these isomers for T_{14} and T_{16} obtained at some calculational levels are shown in Table 4. At all levels of theory, the most stable isomer of T_{14} has the D_{3h} ($6^05^64^3$) symmetry, whereas D_{4d} ($6^05^84^2$) for T_{16}. In contrast, the least stable isomer of T_{14} is the second D_{3h} ($6^35^04^6$) and the D_{2d} ($6^45^04^6$) structure for T_{16}, respectively. The stability of the cage increases as the number of the 6-membered ring decreases.

According to the previous DFT study (LDA and NLDA levels) for $[HSiO_{1.5}]_n$ (n = 4, 6, 8, 10, 12, 14, and 16),[10b] the relative stability of T_{14} is the same as ours. However, the most stable isomer of T_{16} is C_{3v} at the LDA, whereas D_{2d} is most stable at the NLDA level; the results of LDA and NLDA are different for the most stable isomer of T_{16}. Furthermore, another DFT study (GGA with DNP) of methyl silsesquioxanes, $[MeSiO_{1.5}]_n$ (n = 4, 6, 8, 10, 12, 14, and 16),[10c] reported the same conclusion as ours for T_{14} but C_{3v} ($6^15^64^3$) type of the structure as the most stable isomer of T_{16}. Therefore, there are discrepancies for the stability of the isomers of T_{16}. However, given that the experimental study on the $^{29}Si\{^1H\}$ NMR chemical shift[10a] observed the structure with D_{4d} symmetry for T_{16}, and for the relation of the number of 6-membered ring and stability, the same trend is seen in T_{14} and T_{16}, we think our result seems to be reasonable.

For the insertion of H_2 into all isomers of T_{14} and T_{16}, we will begin our discussion by considering the geometrical change of the cages and H_2 molecule on the reaction. For the cages, the same trend as that in the smaller T_8 has been observed in all cases investigated here. That is, on the face where the H_2 molecule inserts, the Si—O bond length increases, the Si—O—Si bond angles become narrow while the O—Si—O bond angles widen in the transition structure but other parts of the molecule are almost unchanged. Furthermore, in the inclusion complex, the geometrical change that happened in the transition structure has disappeared. In particular, as the size of the cage becomes large, the effect of the incorporation of an H_2 molecule on the geometry seems to be negligible.

On the other hand, the bond distance of H_2 in T_{14} (complex) is 0.730−0.731 Å, whereas that in T_{16} is 0.732−0.733 Å, which is longer than those in the substituted T_8. It becomes close to that (0.734 Å) in a free H_2 molecule, probably because of the large space of T_{14} and T_{16}. As seen from these results, the effect of the insertion on the geometry of the cage and H_2 molecule are smaller compared to the smaller T_8.

Table 5 summarizes the energetics of the various cases of the insertion of H_2 into T_{14} and T_{16}. R_n (n = 4−6) in the table indicates the face on which the insertion takes place, as seen from Figures 4 and 5. For the most stable D_{3h} isomer of T_{14}, we have examined two cases of insertion reaction; one is from R_5 (D_5) and another from R_4 (D_4). The systems are so big that even the MP2 single point energy calculations with the TZV(d,p) basis set were not at present possible here. However, as mentioned before, we have found the MP2/SBK energies are good estimations of the MP2/TZV(d,p) energies. For both sizes of POSS, the energy barrier increases in the order $R_6 < R_5 < R_4$, the size of the face where the H_2 insertion takes place

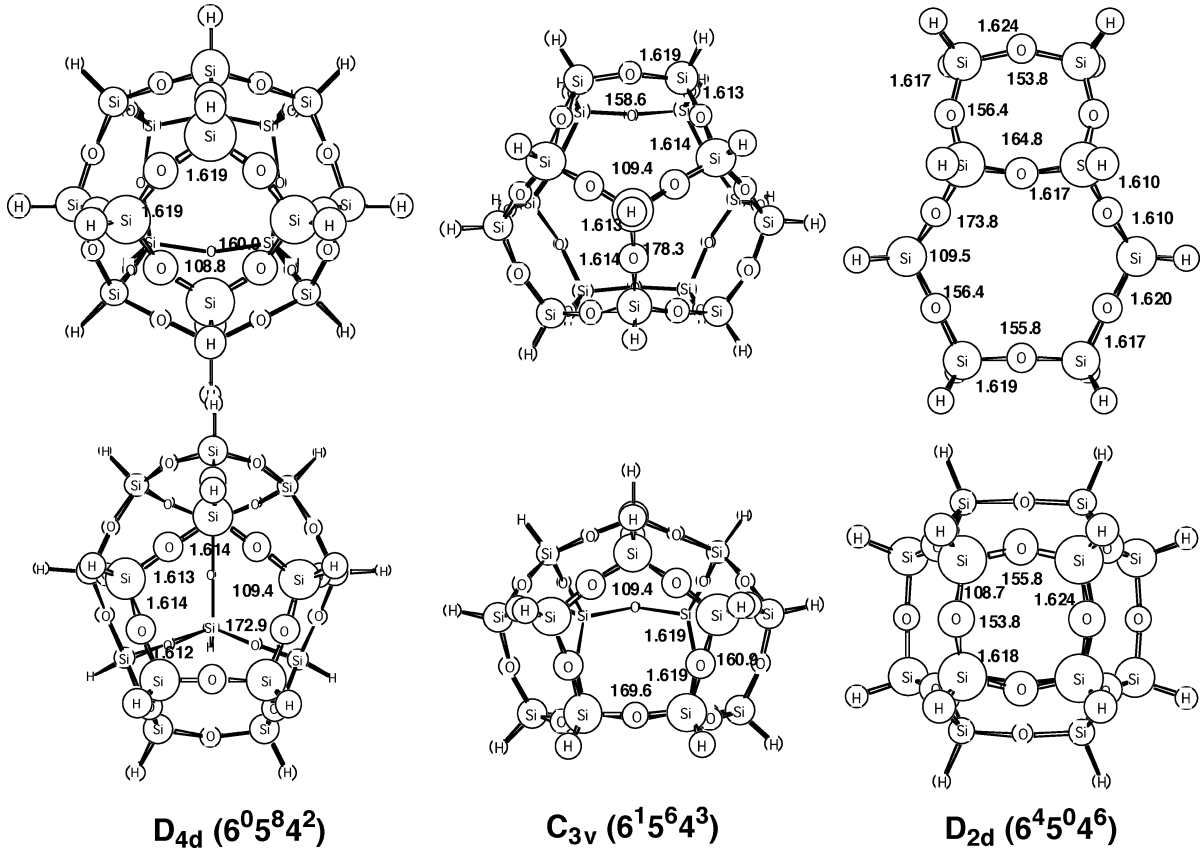

Figure 5. HF/TZV(d,p) optimized geometries (Å and degrees) of the three isomers of T_{16} in two different views.

TABLE 4: Relative Energies (kcal/mol) of the Three Isomers of T_n-POSS (n = 14 and 16) at the HF/TZV(d,p) and MP2/SBK Levels of Theory

	HF/TZV(d,p)	MP2/SBK
T_{14}		
D_{3h} ($6^0 5^6 4^3$)	0	0
C_{2v} ($6^1 5^4 4^4$)	2.4	5.2
D_{3h} ($6^3 5^0 4^6$)	7.6	14.7
T_{16}		
D_{4d} ($6^0 5^8 4^2$)	0.0	0.0
C_{3v} ($6^1 5^6 4^3$)	1.9	4.8
D_{2d} ($6^4 5^0 4^6$)	8.1	17.9

TABLE 5: Energy Barriers (kcal/mol) for the Insertion of H_2 into the Three Isomers of T_n-POSS (n = 14 and 16) from the R_4, R_5, and R_6 Faces and the Energies of the Inclusion Complex (kcal/mol) Relative to the Reactants at the HF/TZV(d,p) and MP2/SBK Levels of Theory

	energy barrier		stabilization energy of the complex	
	HF/TZV(d,p)	MP2/SBK	HF/TZV(d,p)	MP2/SBK
T_{14}				
D_{3h} (R_5)	33.5	22.9	1.8	−0.7
(R_4)		73.2	same as R_5	same as R_5
C_{2v} (R_6)	11.4	5.8	1.9	−0.7
D_{3h} (R_6)	12.7	6.8	2.7	−0.4
T_{16}				
D_{4d} (R_4)	93.5	72.9	1.0	−0.9
C_{3v} (R_6)	10.9	5.5	0.5	−1.2
D_{2d} (R_4)	93.8	73.7	1.4	−1.0

decreases. As demonstrated in the D_{3h} isomer of T_{14}, the H_2 may choose the larger faces to insert among the different size of faces. This is not only the same trend as that in the smaller POSS (T_6, T_{10}, and T_{12}), but also the energy values are also very similar,[13] suggesting again that the energy barrier depends just on the size of the face and not on the cage size.

However, we have found that the size of the cage plays an important role in the stabilization energy of the inclusion complex. As seen from the table, the MP2/SBK stabilization energies are negative in all cases, while the corresponding values at the HF/TZV(d,p) are positive. Nevertheless, all numbers are very small compared to the case of the smaller POSS, so it is apparent that the H_2 encapsulation does not have significant effect on the stability of these sizes of POSS. The stabilization energies in T_{16} are, however, slightly larger than those in T_{14}. The inclusion of the molecule seems to be much easier in the larger POSS, as expected. Furthermore, "same as R_5" in the case of the insertion from R_4 of the D_{3h} isomer of T_{14} suggests that the H_2 molecule can move to the better position inside of the cage (see Figure 6). This may be harder in the smaller POSS. As a result, the POSS with larger cage size is expected to include the hydrogen molecules without much difficulty and the encapsulated H_2 moves easily compared to the smaller POSS.

3. Inserting Multiple H_2 Molecule into T_{14} and T_{16}. We have emphasized many times that the size of the cage is very important for the stability of the inclusion complex, but in addition to the size, the shape of the cage is also found to be important. In the previous study, we reported that the encapsulation of *two* H_2 molecules is possible in T_{10} but not in T_{12} (D_{6h}) in spite of the larger D_6 faces, which is favorable for the insertion of the H_2 molecule.[3i] This may be explained from the fact that the height of the prism in T_{12} (D_{6h}) is lower than that in T_{10}, so one H_2 molecule may be pushed out easily. Therefore, we have tried to examine the case of the D_{2d} isomer of T_{12} with the more complicated shape than D_{6h} in this study. As shown in Figure 7, the D_{2d} isomer can absorb two H_2 molecules inside. Furthermore, another important point is that the first H_2 changes the direction at the second

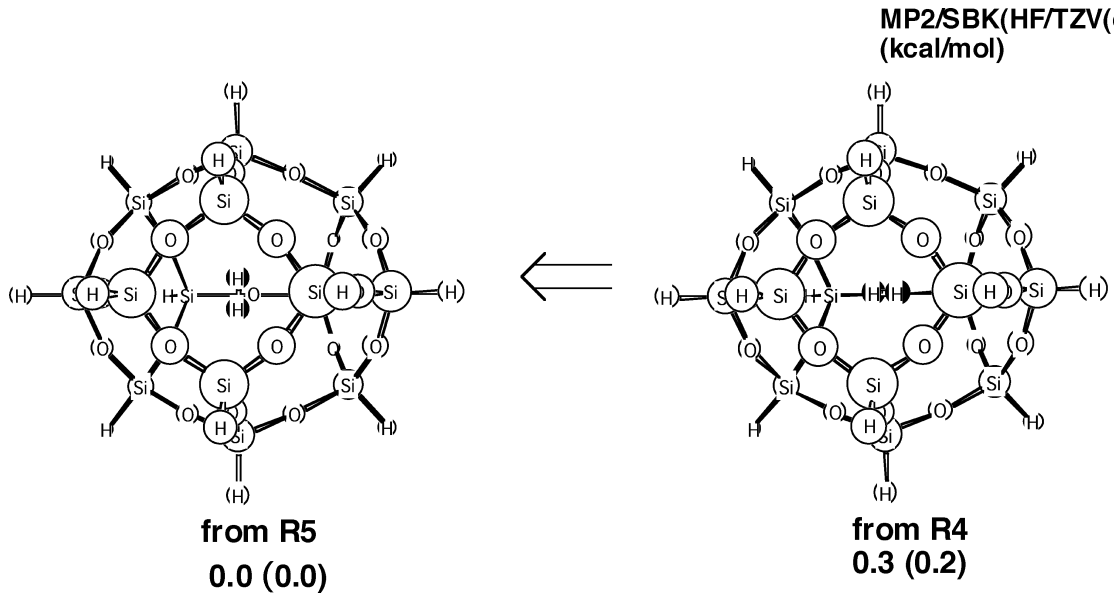

Figure 6. The two kinds of the inclusion complex of T_{14} (D_{3h}) in which the H_2 insertion took place at the different face (R_4 and R_5). The values are the relative energies at the MP2/SBK and HF/TZV(d, p) levels of theory.

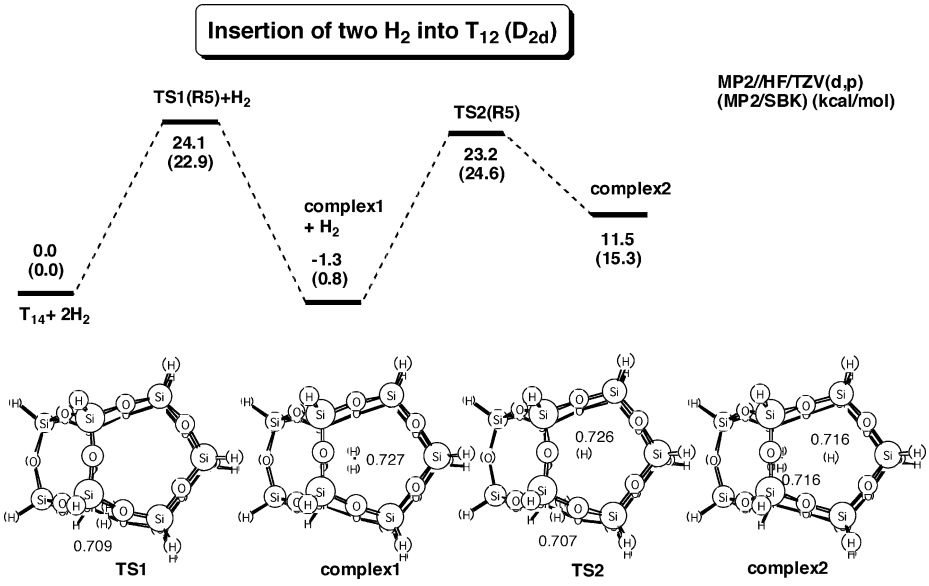

Figure 7. MP2/TZV(d,p)//HF/TZV(d,p) and MP2/SBK potential energy surface (kcal/mol) for the two H_2 insertions into T_{12} (D_{2d}) in a stepwise manner. The numbers in the molecular structures are the bond length of H_2 (Å).

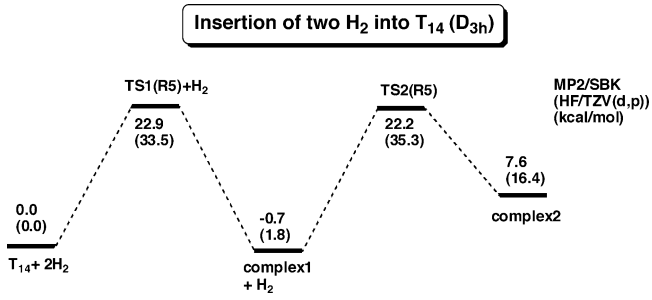

Figure 8. HF/TZV(d,p) and MP2/SBK potential energy surface (kcal/mol) for the two H_2 insertions from R_5 into T_{14} (D_{3h}) in the stepwise manner.

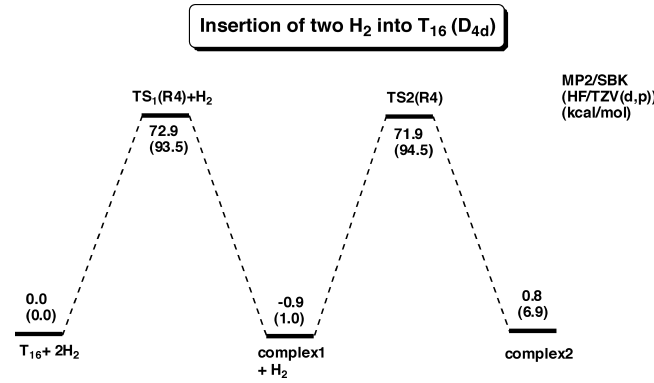

Figure 9. HF/TZV(d,p) and MP2/SBK potential energy surface (kcal/mol) for the two H_2 insertions from R_4 into T_{16} (D_{4d}) in the stepwise manner.

transition state, probably because it is the energetically better position for the insertion of the second H_2.

As seen from Figure 7, the bond length of two H_2 molecules in complex 2 becomes short compared to that in complex 1. From this and the above results, the bond length of the H_2 inside of the cage seems to be strongly affected by the room space.

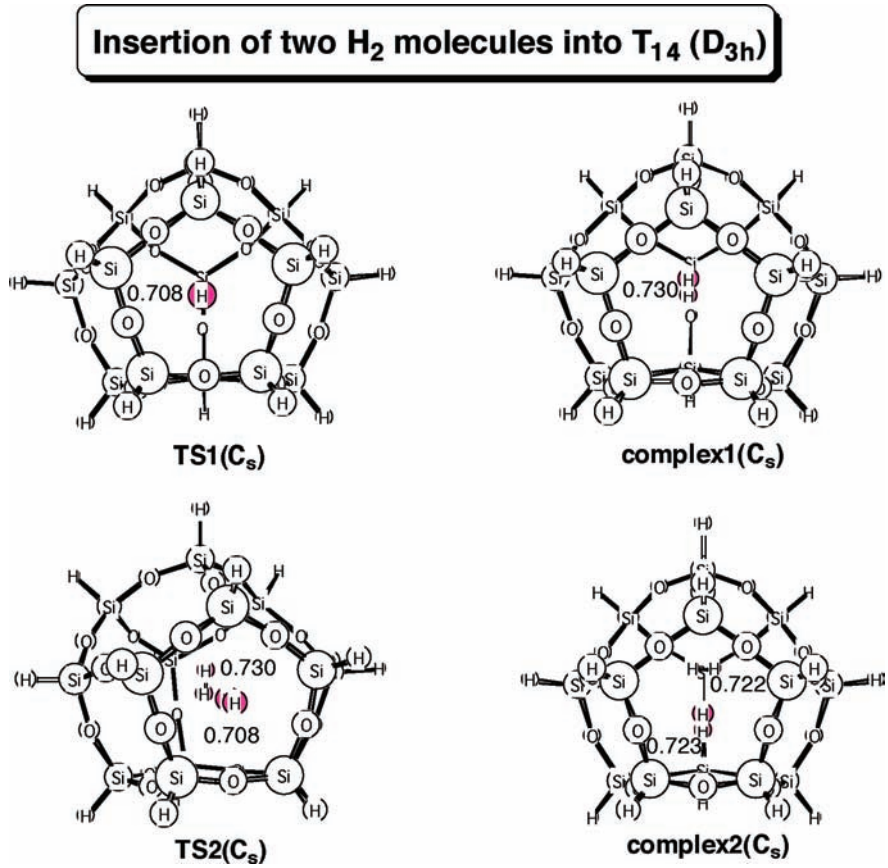

Figure 10. HF/TZV(d,p) optimized structures of four stationary points on the potential energy surface for the two H_2 insertions into T_{14} (D_{3h}) in the stepwise manner. The numbers in the molecular structures are the bond length of H_2 (Å).

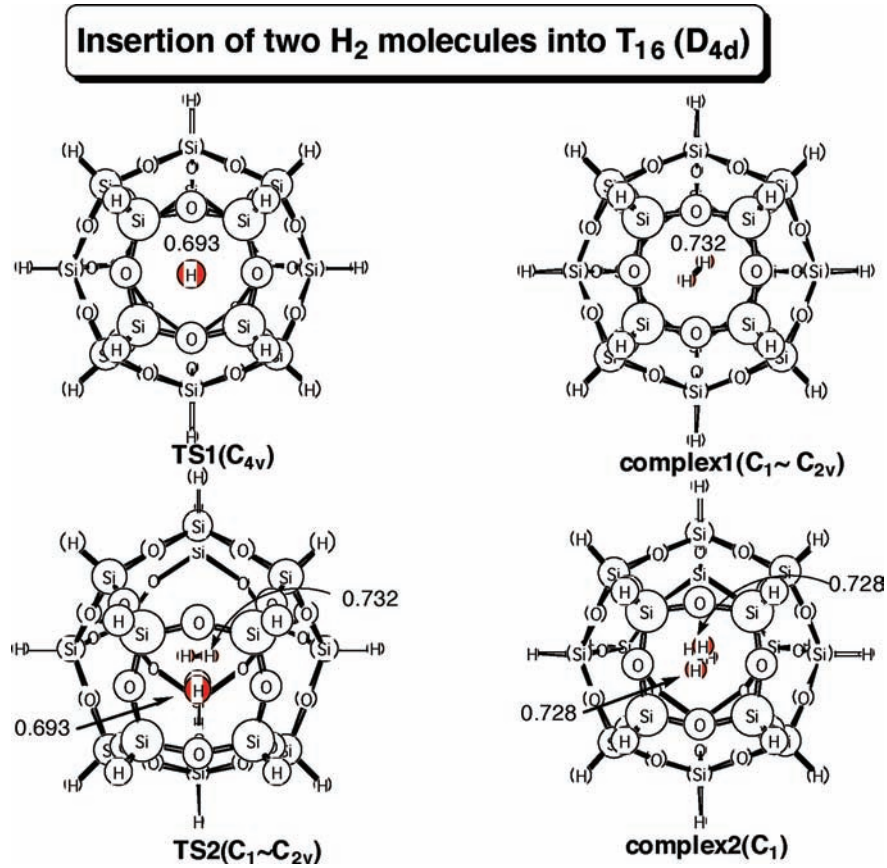

Figure 11. HF/TZV(d,p) optimized structures of four stationary points on the potential energy surface for the two H_2 insertions into T_{16} (D_{4d}) in the stepwise manner. The numbers in the molecular structures are the bond length of H_2 (Å).

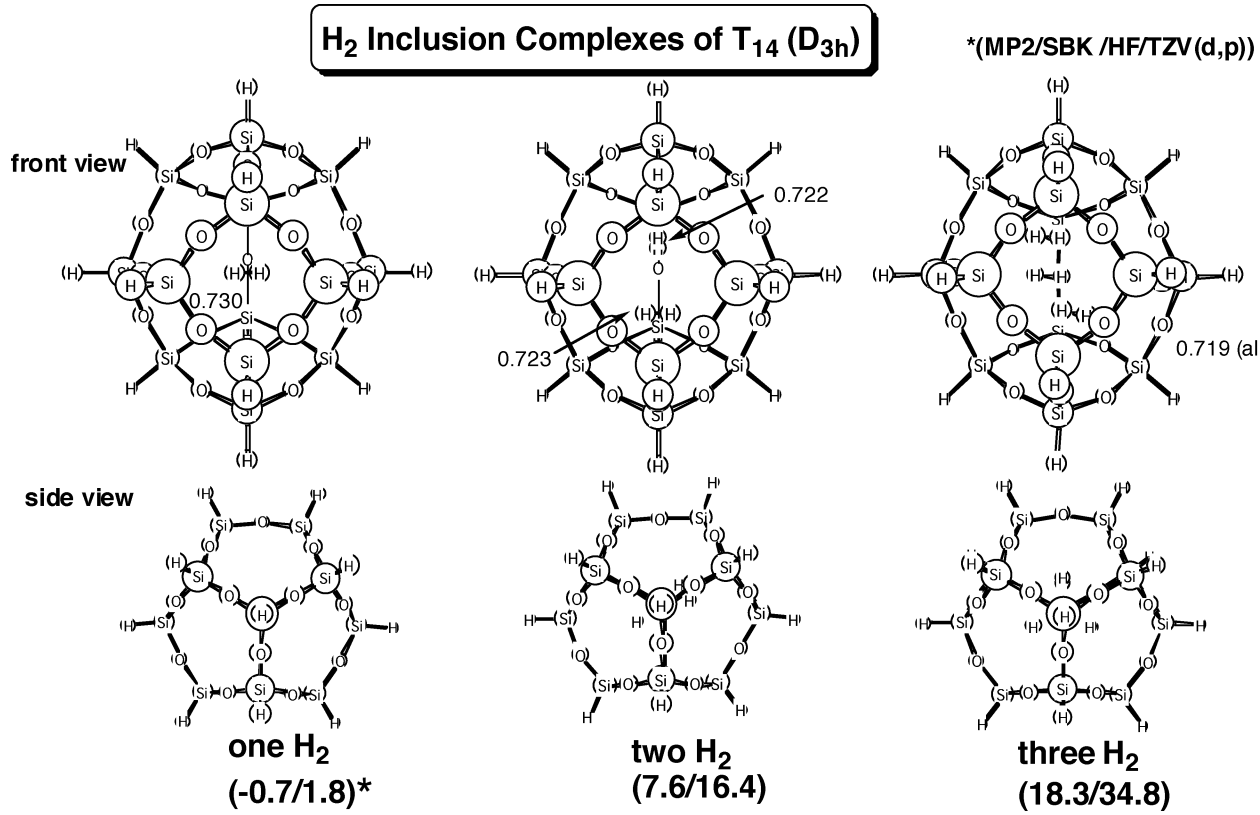

Figure 12. HF/TZV(d,p) optimized structures of three inclusion complexes of $T_{14}(D_{3h})$ with one through three H_2 molecules and the energies (kcal/mol) relative to the isolated hydrogen molecules (one through three) and $T_{14}(D_{3h})$ at the MP2/SBK and HF/TZV(d,p) levels of theory. The numbers in the molecular structures are the bond length of H_2 (Å).

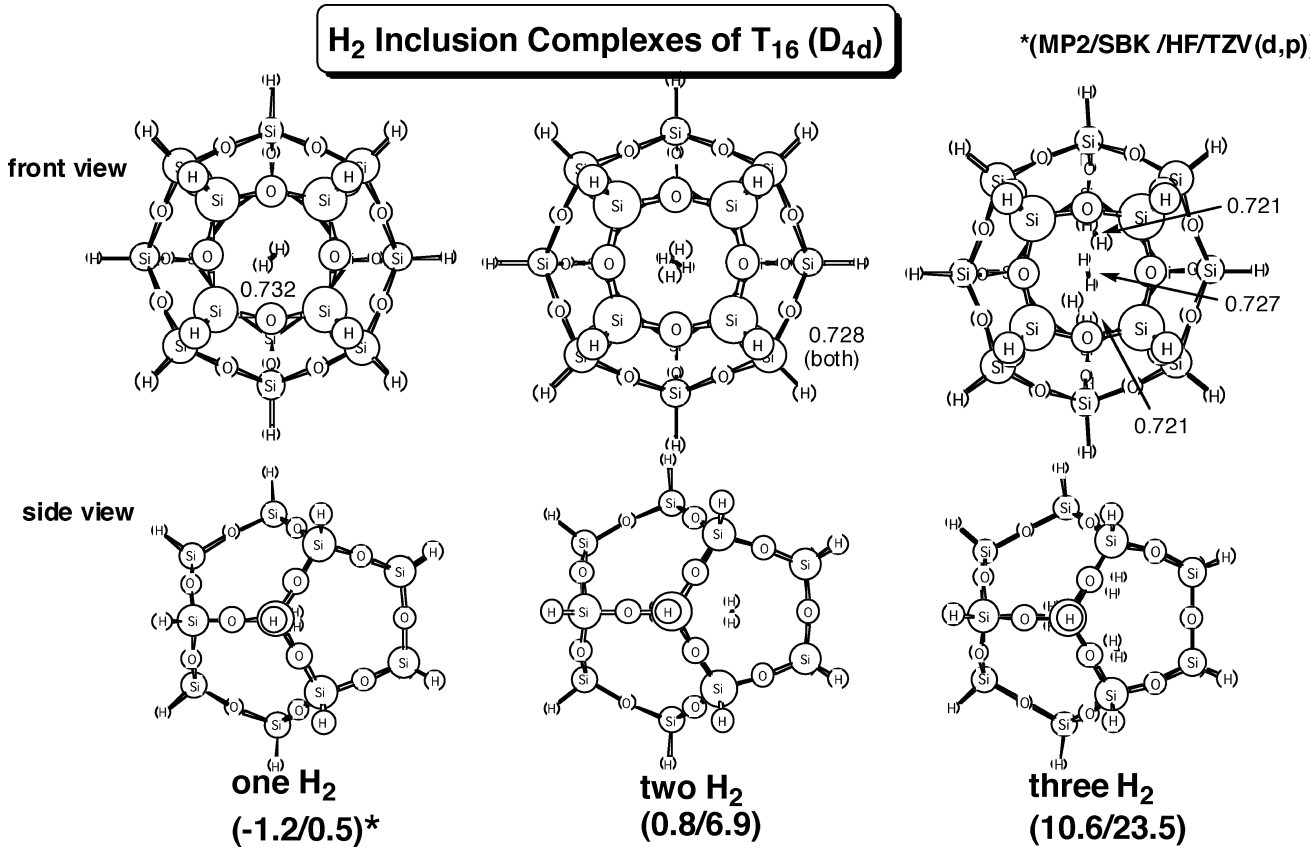

Figure 13. HF/TZV(d,p) optimized structures of three inclusion complexes of $T_{16}(D_{4d})$ with one through three H_2 molecules and the energies (kcal/mol) relative to the isolated hydrogen molecules (one through three) and $T_{16}(D_{4d})$ at the MP2/SBK and HF/TZV(d,p) levels of theory. The numbers in the molecular structures are the bond length of H_2 (Å).

As a result, in addition to the size of the cage, the complicated shape seems to be the key to keep more than one H_2 molecule.

Next, we consider the encapsulation of multiple H_2 molecule in the larger POSS compounds (T_{14} and T_{16}). These POSS are not only bigger than T_{12} but also have relatively complicated polyhedral structures compared to prisms, which are good conditions to keep multiple H_2 molecules in the cage. The potential energy surfaces of the stepwise insertion of two H_2 molecules into the most stable isomer of T_{14} (D_{3h}) and T_{16} (D_{4d}) are displayed in Figures 8 and 9, respectively, and the HF/TZV(d,p) optimized geometries of the transition states and inclusion complexes are shown in Figures 10 and 11. Again, the geometrical changes on the cages are quite local for both cases. It is obvious that the first included H_2 rotates to make more space for the second H_2 at the second transition state in both cases. Furthermore, the bond length of the H_2 molecule becomes short as the number of the H_2 in the cage increases. These phenomena are also seen in the smaller D_{2d} isomer of T_{12} as already mentioned.

Compared to T_{14}, T_{16} shows much higher energy barriers as the H_2 molecules insert from D_4 (R_4) but the complexes are more stable compared to the T_{14} case because of the larger room.[14] The energy barriers for the first and second insertions are almost similar for both cases. In addition, for T_{16}, the stabilization of the second inclusion complex is also the same as the first one, suggesting that the room of T_{16} is large enough to include two hydrogen molecules.

On the basis of these results, we finally have tried to incorporate the third H_2 molecule in T_{14} and T_{16}. In Figures 12 and 13 are shown the optimized geometries of the one through three H_2 inclusion complexes for T_{14} and T_{16}, respectively. From the figures, we can see that the previously included hydrogen molecules change the position to make more room for the next coming hydrogen molecule. The number of H_2 molecules increase, the bond distance of H_2 becomes shortened, and the inclusion complex is destabilized, as expected. However, the destabilization energy of T_{16} complex is smaller than those of T_{14} compound.

The way of the interaction of hydrogen molecules encapsulated should be noted here. In both POSS and $T_{12}(D_{2d})$, each H_2 molecule takes the cross position with some distance when two molecules are included. However, if the third hydrogen came, the three molecules align in roughly parallel manner. In the two H_2 encapsulated complex, the distance[15] of two H_2 molecules is 2.220 Å for T_{14} and 2.488 Å for T_{16}, respectively, whereas that in $T_{12}(D_{2d})$ is 2.082 Å. Furthermore, if you will have one more H_2 in T_{14} and T_{16}, the distances among three H_2 molecules are 2.293, 2.293, and 2.238 Å for T_{14} and 2.546, 2.546, and 2.290 Å for T_{16}, respectively. Interestingly, two of them seem to interact strongly compared to the others.

Incidentally, the average Mulliken charges on each H_2 molecule in T_{14} and T_{16} are as follows: −0.0472 (one H_2 in T_{14}), −0.0482 (two H_2 in T_{14}), −0.0554 (three H_2 in T_{14}), −0.0352 (one H_2 in T_{16}), −0.0370 (two H_2 in T_{16}), and −0.0449 (three H_2 in T_{16}). All values are more positive and close to the electrically neutral condition compared to the case of T_8. However, it is interesting to note that the negative charge on each H_2 molecule increases as the cage is crowded.

The present study shows that the larger POSS such as T_{14} and T_{16} seem to be able to absorb at least two or three hydrogen molecules without much difficulty, compared to the smaller POSS. Furthermore, the complicated polyhedral structures are expected to be favorable to keep the molecules inside of the cage. In conclusion, therefore, the larger POSS are promising candidates as H_2 storage materials, although much more investigation is necessary to extend the present results to the treatment of hydrogen gas.

Conclusions

As a continuation of our study on H_2 insertion reactions into various POSS and to supply more information regarding the possibility of POSS as an H_2 storage material, the mechanisms of the H_2 encapsulating reaction for the substituted T_8 and larger POSS, T_{14}, and T_{16}, were investigated.

We already have found that the energy barrier of the reaction depends on the size of the face where an H_2 inserts in our previous study. In agreement with this conclusion, for the H_2 insertion reaction of the substituted T_8, the substituents which make the SiO bond longer by any reasons tend to lower the energy barrier for insertion, whereas those with the opposite effect make the barrier higher compared to the case of the H-substituted T_8, $[HSiO_{1.5}]_8$. This means that we can control the reaction with substituents to some extent. Also, it may be noteworthy that the lithium analog, $[LiSiO_{1.5}]_8$, is found to have very unique equilibrium structures with lithium atoms bridging over the silicon and oxygen atoms of the framework, and the structure is markedly stable in energy compared to that of the normal H analog.

For the stability of three isomers of T_{14} and T_{16}, our results show that the number of the 6-membered rings decreases, the stability of isomers increases in both POSS. Furthermore, in these POSS, it is possible encapsulate multiple hydrogen molecules, due to the larger and complicated shape of the cages compared to the smaller POSS ($n < 10$). The encapsulated H_2 can move easily inside of these large POSS. In conclusion, the present results suggest that the larger POSS is a good H_2 carrier, although more investigation may be necessary to determine the maximum number of H_2 molecules that can possibly be encapsulated and further elucidate the treatment of hydrogen gas.

Acknowledgment. This work has been supported by a Grant-in-Aid on Priority-Area-Research: Molecular Theory for Real Systems (461).

Supporting Information Available: The HF/TZV(d,p) optimized geometries of three isomers of T_{14} and T_{16}. This information is available free of charge via the Internet at http://pubs.acs.org.

References and Notes

(1) See, for example: (a) Voronkov, M. G.; Lavrent'yev, V. L. *Top. Curr. Chem.* **1982**, *102*, 199. (b) Feher, F. J.; Newman, D. A.; Walzer, J. F. *J. Am. Chem. Soc.* **1989**, *1111*, 1741. (c) Baney, R. H.; Itoh, M.; Sakakibara, A.; Suzuki, T. *Chem. Rev.* **1995**, *95*, 1409. (d) Feher, F. J.; Budzichowski, T. A. *Polyhedron* **1995**, *14*, 3239.

(2) For the effect of the fluorine substitution on POSS, see: Mabry, J. M.; Vij, A.; Iacono, S. T.; Viers, B. D. *Angew. Chem., Int. Ed.* **2008**, *47*, 4137.

(3) (a) Tejerina, B.; Gordon, M. S. *J. Phys. Chem. B* **2002**, *106*, 11764. (b) Villaescusa, L. A.; Lightfoot, P.; Morris, R. E. *Chem. Commun.* **2002**, 2220. (c) Bassindale, A. R.; Pourny, M.; Taylor, P. G.; Hursthouse, M. B.; Light, M. E. *Angew. Chem., Int. Ed.* **2003**, *42*, 3488. (d) Park, S. S.; Xiao, C.; Hagelberg, F.; Hossain, D.; Pittman, C. U., Jr.; Saebo, S. *J. Phys. Chem. A* **2004**, *108*, 11260. (e) Satre, G.; Pulido, A.; Corma, A. *Chem. Commun.* **2005**, 2357. (f) Pach, M.; Macrae, R. M.; Carmichael, I. *J. Am. Chem. Soc.* **2006**, *128*, 6111. (g) Tossell, J. A. *J. Phys. Chem. C* **2007**, *111*, 3584. (h) Hossain, D.; Pittman, C. U., Jr.; Saebo, S.; Hagelberg, F. *J. Phys. Chem. C* **2007**, *111*, 6199. (i) Kudo, T.; Akasaka, M.; Gorond, M. S. *Theor. Chem. Acc.* **2008**, *120*, 155. (j) Anderson, S. E.; Bodzin, D. J.; Haddad, T. S.; Boatz, J. A.; Mabry, J. M.; Mitchell, C.; Bowers, M. T. *Chem. Mater.* **2008**, *20*, 4299. (k) Hossain, D.; Pittman, C. U., Jr.; Hagelberg, F.; Saebo, S. *J. Phys. Chem. C* **2008**, *112*, 16070. (l) Hossain,

D.; Gwaltney, S. R.; Pittman, C. U., Jr.; Saebo, S. *Chem. Phys. Lett.* **2009**, *467*, 348. (m) Geoge, A. R.; Catlow, C. R. A. *Chem. Phys. Lett.* **1995**, *247*, 408.

(4) Kudo, T.; Shima, N.; Iimura, T., manuscript in preparation.

(5) (a) Kudo, T.; Gordon, M. S. *J. Am. Chem. Soc.* **1998**, *120*, 11432. (b) Kudo, T.; Gordon, M. S. *J. Phys. Chem. A.* **2000**, *104*, 4058. (c) Kudo, T.; Gordon, M. S. *J. Phys. Chem. A.* **2002**, *106*, 11347. (d) Kudo, T.; Machida, K.; Gordon, M. S. *J. Phys. Chem. A.* **2005**, *109*, 5424. (e) Kudo, T.; Gordon, M. S. *J. Phys. Chem. A.* **2001**, *105*, 11276. (f) Kudo, T.; Gordon, M. S. *J. Phys. Chem. A.* **2003**, *107*, 8756. (g) Kudo, T.; Akasaka, M.; Gordon, M. S. *J. Phys. Chem. A* **2008**, *112*, 4836.

(6) Pople, J. A.; Seeger, R.; Krishnann, R. *Int. J. Quantum Chem.* **1979**, *S11*, 149.

(7) (a) Stevens, W. J.; Basch, H.; Krauss, M. *J. Chem. Phys.* **1984**, *81*, 6026. (b) Stevens, W. J.; Krauss, M.; Jasien, P. *Can. J. Chem.* **1992**, *70*, 612. (c) Cundari, T. R.; Stevens, W. J. *J. Chem. Phys.* **1993**, *98*, 5555.

(8) (a) Wachters, A. J. H.*J. Chem. Phys.* **1970**, *52*, 1033. (b) Rappe, A. K.; Smedley, T. A.; Goddard, W. A., III*J. Phys. Chem.* **1981**, *85*, 2607.

(9) (a) Schmidt, M. W.; Baldridge, K. K.; Boatz, J. A.; Elbert, S. T.; Gordon, M. S.; Jensen, J. H.; Koseki, S.; Matsunaga, N.; Nguyen, K. A.; Su, S.; Windus, T. L.; Dupuis, M.; Montgomery, J. A., Jr. *J. Comput. Chem.* **1993**, *14*, 1347. (b) Gordon, M. S.; Schmidt, M. W. *Advances in Electronic Structure Theory: GAMESS a Decade Later, Theory and Applications of Computational Chemistry*; Dykstra, C. E.; Frenking, G.; Kim, K. S.; Scuseria, G. E. Eds.; Elsevier: New York, 2005; Ch. 41.

(10) (a) Agaskar, P. A.; Klemperer, W. G. *Inorg. Chim. Acta* **1995**, *229*, 355. (b) Xiang, K.-H.; Pandey, R.; Pernisz, U. C.; Freeman, C. *J. Phys. Chem. B* **1998**, *102*, 8704. (c) Franco, R.; Kandalam, A. K.; Pandey, R.; Pernisz, U. C. *J. Phys. Chem. B* **2002**, *106*, 1709.

(11) Early, C. W. *J. Phys. Chem.* **1994**, *98*, 8693.

(12) Kudo, T.; Hashimoto, F.; Gordon, M. S. *J. Comput. Chem.* **1996**, *17*, 1163.

(13) The MP2/SBK energy barriers are 71.1−74.3 kcal/mol for R_4, 22.1−22.9 kcal/mol for R_5, and 4.1 kcal/mol for R_6, respectively.

(14) The reason why we have investigated the H_2 insertion from the smaller face (R_4) instead of R_5 is that the D_{4d} conformer has the longer structure in this direction compared to that of R_5, which may be convenient for the continuous insertion of two hydrogen molecules (see Figure 5).

(15) It is the distance between the middle points of each HH bond.

JP904488S